Published in final edited form as:
Phys Biol. 2011 April ; 8(2): 026013. doi:10.1088/1478-3975/8/2/026013.

Engineering strategies to recapitulate epithelial morphogenesis within synthetic 3 dimensional extracellular matrix with tunable mechanical properties

Y.A. Miroshnikova[1,2], **D.M. Jorgens**[4], **L. Spirio**[5], **M. Auer**[4], **A.L. Sieminski-Sarang**[1], and **V.M. Weaver**[2,3]

[1]Olin College of Engineering, Needham, MA, 02492

[2]Department of Surgery, Center for Bioengineering and Tissue Regeneration, University of California, San Francisco, San Francisco, CA, 94143

[3]Departments of Anatomy and Bioengineering and Therapeutic Sciences, Eli and Edythe Broad Center of Regeneration Medicine and Stem Cell Research and Helen Diller Family Comprehensive Cancer Center, University of California San Francisco, San Francisco, CA 94143

[4]Lawrence Berkeley National Laboratory, UC Berkeley, Berkeley, CA, 94720

[5]PuraMatrix/ 3DM Inc., Cambridge, MA, 02142

Abstract

The mechanical properties (e.g. stiffness) of the extracellular matrix (ECM) influence cell fate and tissue morphogenesis and contribute to disease progression. Nevertheless, our understanding of the mechanisms by which ECM rigidity modulates cell behavior and fate remains rudimentary. To address this issue, a number of two and three dimensional (3D) hydrogel systems have been used to explore the effects of mechanical properties of the ECM on cell behavior. Unfortunately, many of these systems have limited application because fiber architecture, adhesiveness and/or pore size often change in parallel when gel elasticity is varied. Here we describe the use of ECM-adsorbed, synthetic, self-assembling peptide gels (SAPs) that are able to recapitulate normal epithelial acini morphogenesis and gene expression in a 3D context. By exploiting the range of visco-elasticity attainable with these SAP gels, and their ability to recreate native-like ECM fibril topology with minimal variability in ligand density and pore size, we were able to reconstitute normal versus tumor-like phenotype and gene expression patterns in nonmalignant mammary epithelial cells (MECs). Accordingly, this SAP hydrogel system presents the first tunable system capable of independently assessing the interplay between ECM stiffness and multi-cellular epithelial phenotype in a 3D context.

Keywords

epithelial morphogenesis; extracellular matrix; self-assembling peptides; biomaterials; mechanical properties; viscoelasticity; tumor

[6]To whom correspondence should be addressed: Valerie M. Weaver, University of California, San Francisco 513 Parnassus Avenue, 565 Health Sciences East San Francisco, CA 94143-0456 Valerie.weaver@ucsfmedctr.org Telephone: 415-476-3973 Fax: 415-476-3985.

Introduction

Cells *in vivo* are constantly exposed to an array of biophysical forces such as hydrostatic pressure, shear stress, compression loading, and tensional forces. Cells rely on these physical cues to maintain homeostasis and adapt to them by altering cell signaling and gene expression and by remodeling their local microenvironment [1–2]. From an organismal point of view, ECM compliance directs the development of tissues [1, 3] and influences the onset of many pathological conditions, including cardiovascular disease [4], arthritis [5] , and neural degenerative diseases [6–7]. The ECM also progressively stiffens in tumors and recent work suggests this phenotype has functional significance because increasing ECM rigidity promotes malignant transformation, while inhibiting ECM stiffening reduces tumor incidence [8–10]. Accordingly, clarifying the role by which ECM compliance influences diverse cellular and tissue level functions is central to understanding the molecular basis for development and organ homeostasis. Nevertheless, the molecular mechanisms whereby ECM compliance regulates cellular behavior and tissue phenotype remain poorly understood.

One frequently employed simplified model system used to study the effect of ECM stiffness on cell behavior is protein-conjugated polyacrylamide gels (PA gels) [11–15]. These nearly elastic 2D gels permit the systematic and predictable modulation of ECM compliance by changing cross-linker concentration while maintaining ligand density and growth factor milieu constant. PA gels have proved quite useful in exploring fundamental links between ECM stiffness and cell behavior, and when used in conjunction with a matrix overlay assay, they have illustrated a role for ECM tension in epithelial morphogenesis [3, 6, 10, 16–20]. These PA gels have also been used to identify molecular mechanisms by which ECM stiffness modulates cell phenotype including highlighting how ECM compliance can regulate cell behavior by influencing integrin adhesions and growth factor receptor signaling [10, 21–24]. Indeed, studies using PA gels have proved instrumental in illustrating how physical cues from the ECM are sensed and propagated and how ECM tension can alter membrane receptor function and nuclear morphology to modify gene expression [25–27]. Yet, most cells exist within the context of a three dimensional (3D) tissue and it is now recognized that dimensionality per se is a profound regulator of cell and tissue phenotype [28–36]. In this regard, PA gels represent a pseudo 3D rigidity assay system because only the basal domain of the cell remains in contact with, and therefore responds to, the elasticity of the protein-laminated PA gel. Moreover, while animal studies have yielded important insight regarding the interplay between ECM topology, and rigidity within a 3D context [10, 35, 37–38] *in vivo* tissues are inherently complex and hence do not lend themselves as readily to rigorous mechanistic manipulations and quantitative analysis. Accordingly, tractable *in vitro* systems are needed with which to study the molecular basis by which ECM stiffness influences cellular fate in the context of a 3D ECM.

A variety of natural matrices, such as Matrigel (rBM), collagen I (col I), and fibrin gels have been exploited with varying degrees of success to explore the effect of ECM stiffness and topology *in vitro* on cellular behavior and fate in a 3D context [39–43]. Using these hydrogel systems gel stiffness has been routinely modulated by altering the concentration or composition of the gel constituents or by varying cross-link density. Such approaches as these however, simultaneously alter gel pore size, fiber architecture, and/or the number or availability of adhesion sites [44–45]. Further, these natural ECM systems frequently display inconsistencies and batch to batch variation. By contrast, synthetic biomaterials promise greater control of mechanical and adhesive properties. In this regard, a variety of approaches have been undertaken to design 3D scaffolds that combine biological functionality and the architecture of natural ECM materials with the robust controllability of synthetic materials. These scaffolds include agarose-stiffened collagen I gels [46], polyethylene glycol (PEG)

gels with tethered adhesion and degradation sites [47–50], as well as a variety of systems with dynamic biophysical and biochemical properties [51–52]. Unfortunately however, many of these gel systems lack the appropriate ECM-like fiber architecture and display limited pore size with increased ECM stiffness.

Self-assembling peptides (SAPs) are a family of 8–32 amino acid peptides that, when exposed to physiological salt solutions, self-assemble into fibrils [53–54]. SAPs are chemically defined and biologically compatible biomaterials that mimic the architectural features observed in some natural matrices such as type I collagen gels [55]. Moreover, SAP family members support cell adhesion and can direct the differentiated behavior of neural stem cells [56], osteoblasts [57], hepatocytes [58–59], and endothelial cells [55]. Motivated by these results we decided to explore the applicability of PuraMatrix, one type of commercially available SAP, to study the interplay between ECM stiffness and MEC morphogenesis in 3D. We determined that laminin-adsorbed (ligation of laminin receptors promotes MEC tissue polarity and differentiation) PuraMatrix SAPs not only support MEC acinar morphogenesis but that stiff SAPs promote an invasive epithelial tumor-like phenotype and do so without significantly changing pore size or gel architecture. Accordingly, we contend that these studies represent the first demonstration of a tractable, well defined hydrogel system that is able to recapitulate the biochemical and micro architectural features of the native normal tissue ECM so that the interplay between ECM compliance and multi-cellular tissue behavior can be studied in a 3D “tissue-like” context.

Methods

1.1. Chemicals and antibodies

We used commercial EHS matrix (Matrigel™; Collaborative Research) for the rBM assays, telopeptide intact type I rat tail collagen (1%; Sigma) for the collagen type I hydrogels and aqueous RAD16-I (1 %; AcN-(RADA)4-CNH2; BD PuraMatrix, Becton Dickinson) for the self assembling peptide gels. Primary antibodies used in these studies included: mouse monoclonal anti-human cleaved caspases-3 (clone E83- 77; Epitomics), E cadherin (clone 36; BD Transduction Laboratories), β4 integrin (clone 3E1; Chemicon) and Ki-67 (clone 7B11; Invitrogen); rat monoclonal anti human β1 integrin (clone AIIB2), and rabbit polyclonal anti human fibronectin I (Millipore) and β-catenin (Sigma). Secondary antibodies used were: Alexa Fluor 488- and 555- and 633-conjugated - anti-mouse, anti rat and anti rabbit IgGs (Molecular Probes). Additional reagents included TRITC-conjugated Phalloidin (Molecular Probes), diaminophenylindole (DAPI; Sigma), laminin (L2020, Sigma), and fetal bovine serum (Invitrogen).

1.2. Cell culture

Human nonmalignant MEC MCF10As were propagated as monolayers on tissue culture plastic and assembled into 3D colonies in either rBM or Collagen/rBM gels, as described [8, 60].

1.3. Cell death stimulation and analysis

MECs grown in rBM for 10–12 days (3D multi-cellular spheroid) were assayed for endogenous cell death via apoptosis through immuno-detection of activated caspase 3 or using a modified Live/Dead assay (Invitrogen). Percent death was quantified as the number of cells stained positive for activated caspase 3 or scored positive for death divided by the total number of cells, as described [34, 61]. The minimum number of cells scored was 200–300 per experimental condition. Cells were visualized using a fluorescence microscope (Nikon Inverted Eclipse TE300 microscope).

1.4. Immunofluorescence analysis

Cells were either triton extracted (0.1% Triton X-100; 5 min) and then fixed or directly fixed using paraformaldehyde (4%; Electron Microscopy Sciences). Specimens were thereafter incubated with primary antibody, followed by either Alexa Fluor 488 or 568–conjugated secondary antibody. Nuclei were counterstained with DAPI or Hoechst 33342. Cells were visualized using a Zeiss Laser Scanning Confocal microscope attached to a Nikon Diaphot 200 microscope. Images were recorded at 600X magnification.

1.5. Three dimensional culture within self-assembling peptides

To assay for growth within a 3D SAPs gel, trypsinized MECs (0.05%; trypsin/EDTA; Invitrogen) were washed and re-suspended in sterile 20% sucrose containing either laminin (100 μg/mL; Sigma L2020) or rBM (Matrigel; 2 mg/mL protein; Becton Dickinson). The cell suspension (2X final desired cell concentration) was then combined 1:1 with a 2X solution of self-assembling peptide (from 1% w/v sonicated peptide stock) to attain a final cell concentration of $1X10^5$ cells/mL. 200 μl of the cellular-ECM mixture was thereafter aliquoted into inserts (PICM-012-50, Millipore) and gelation was induced by exposure to cell culture medium (DMEM F-12, 10% FBS, pH 7.4; Invitrogen). After 1 hour, the gelation medium was decanted and replaced with MEC growth medium. Cultures were typically fed every other day and maintained for 18 days.

1.6. Scanning Electron Microscopy

Cell-free collagen and self-assembling peptide gels were fixed in Jonson's reagent (24 hours; 4C; Electron Microscopy Sciences) and cut into 4–5 smaller gels prior to further processing and staining to increase the number of exposed surfaces. After fixation samples were rinsed (3X; 10 minutes; RT; 0.1M sodium cacodylate buffer, pH 7.2;Tousimis), stained with 1% osmium tetroxide (1 hour; RT), and rinsed with 0.1M sodium cacodylate buffer (3 X; 5 minutes; RT). Samples were then subjected to ascending alcohol dehydration, followed by critical point drying procedure with a AutoSamdri 815 CPD critical point dryer (Tousimis). Samples were then transferred onto carbon-taped SEM stubs, sputter coated (Tousimis) with gold palladium and imaged with a Hitachi S-500 scanning electron microscope operated at 30 kV (resolution 3-5nm).

1.7. Rheometry

Cell-free self-assembling peptides, and collagen/rBM gels of varying concentration were gelled in cylindrical molds (~7.5 mm ID), attached to 10% FBS/PBS-wetted parchment paper, polymerized at physiological conditions (48 hours; 37C), released from molds, and transferred to a rheometer with an 8mm plate (AR 2000ex ,TA Instruments)[55]. The shear modulus (G_0) was recorded at a constant frequency of 1 rad/sec for all samples; TA Instruments software accompanying the rheometer was used to fit all data and extract shear moduli from raw data (n=5 gels for all conditions).

1.8. Extracellular Matrix fibril quantification and Data Analysis

Projected fiber diameter and pore size were measured from the SEM images (five representative 60,000X images/each concentration of collagen and SAP) using Image J. Projected pore size was quantified via averaging two diagonals of every pore with clear edges on the SEM images. Projected fiber diameter was quantified by averaging measurements of at least 100 fibers/SEM image. Colony area was traced and analyzed in ImageJ (n=50 acini/condition).

1.9. Statistical analysis

Statistical significance was assessed by performing 1/2-tailed student t-tests. *P* values of less than 0.05 were considered to be significant as indicated by a * symbol in text and graphs, unless otherwise specified.

1.10. Quantitative PCR

RNA was isolated using phenol-choroform extraction and total RNA for each sample was reverse transcribed using random primers (Amersham Biosciences). 18S rRNA primers run in parallel were used as controls. Quantitative PCR reactions (10 μl) were conducted using a LightCycler (Roche Diagnostics) with a LightCycler Fast Start DNA Master SYBR Mix (Roche) and a 1 pmol primer mixture.

Results

Increasing Collagen Concentration and Rigidity Stimulate Epithelial Growth and Survival and Compromise Tissue Morphogenesis and Integrity

Primary and immortalized MECs have been used to study the role of the ECM and its receptors in tissue morphogenesis and differentiation. When incorporated into a 3D rBM (Matrigel) human and murine MECs assemble into growth-arrested, polarized multi-cellular structures that resemble terminal ductal lobular units of the *in vivo* mammary gland [31, 39]. MECs will also assemble into non-polarized 3D organoids when grown within type I collagen gels and can be induced to polarize if either purified laminin or rBM (2 mg/ml) is added [62].

The viscoelasticity of collagen I gels is proportional to their concentration. As such collagen gels provide an attractive system with which to study the effect of modulating ECM stiffness in a 3D context on tissue behavior. Accordingly, to study the effect of modulating ECM rigidity on epithelial behavior we generated type I collagen gels ranging from 1.2 to 3.2 mg/ml incorporating rBM (Col/rBM cultures; 2 mg/ml) as a polarity cue. We showed previously that these concentrations of collagen achieve gel stiffness that recapitulates the visco-elasticity typically found in a normal, pre malignant and early invasive tumorigenic human and mouse breast [8, 10] [63]. We then assayed for the effect of varying ECM stiffness in a 3D context on the growth and survival and morphogenesis of the nonmalignant human MEC line MCF10A, an immortalized human MEC line that undergoes multi-cellular epithelial morphogenesis in response to compliant 3D rBM cues [10].

Similar to what we and others observed previously, although the nonmalignant MECs incorporated into highly compliant Col/rBM gel (156 Pa ± 42 Pa) grew rapidly for the first six days, by day 10 they assembled growth-arrested acini as indicated by colonies with persistent diameters of 60.2 ± 5.4 μm, (Fig 1A; DIC image; Fig 1C). After 10 days of culture mammary acini in the compliant gels (1.2 mg/mL) also showed evidence of cleared lumens (see arrow figure 1A DIC, top and immunofluoresence, bottom) and achieved apical-basal polarity as demonstrated by basal deposition of laminin and apical-basal localization of β1 integrin (Fig 1A; lower left hand panel). By contrast, even moderate stiffening (2.2 mg/mL) of the Col/rBM (457 ± 67.3 Pa) significantly increased colony size suggestive of elevated cell proliferation (116.5 ± 24.2 μm; Fig 1A DIC top middle panel , Fig 1C). Yet, when gel stiffness approached that quantified in the stroma surrounding a pre-malignant breast epithelium [10], luminal clearing was compromised, indicative of enhanced cell survival (Fig 1B). Furthermore, a collagen stiffness approaching 800–1000 Pascals, similar to that measured in the ECM surrounding early invasive breast lesions, significantly disrupted apical-basal polarity, as revealed by diffuse localization of laminin V and relocalization of β1 integrin along the basal domain of the colony (Fig 1, bottom middle

panel). Intriguingly, not only did MECs embedded within Col/rBM gels with ECM stiffness approaching that measured in breast tumors (1411 ± 350.3 Pa) grow quite large (161.3 ± 21.1 μm; Fig 1C) and form highly disorganized, nonpolar colonies that lacked lumens (Fig 1A; lower panel right and Fig 1B) but these colonies also showed a propensity to form membrane protrusions that projected into the surrounding ECM, consistent with the notion that ECM stiffness promotes a tumor-like phenotype. Importantly however, despite these provocative findings, none of the nonmalignant MECs from the mammary colonies assembled within the rigid rBM/collagen I gels invaded into the gels (Fig 1A DIC top right).

Thus far our findings were consistent with the notion that ECM stiffness compromises epithelial morphogenesis and tissue integrity and induces a "tumor-like" phenotype even in nontransformed epithelial cells. Nevertheless, we noted that interpretation of data obtained with these gels was complicated by the fact that collagen ligand available to bind to cell surface receptors including integrins and discoidin receptors also significantly increased when the gel concentration was increased to stiffen the ECM. Moreover, SEM analysis revealed that the projected pore size and fiber thickness also changed dramatically as the concentration of the collagen gel was progressively increased (Fig 2A). Because ligand binding and pore size can significantly modify cell invasion, these findings indicate that studies aimed at assessing the interplay between ECM stiffness and cell invasion may be compromised using this approach. Furthermore, matrix topology per se can significantly modulate cellular phenotype further complicating the interpretation of experiments conducted using this gel system [46, 64] [65–67]. Thus, these results emphasize that it is still not clear if ECM stiffness per se can induce invasion of non-transformed epithelial tissues. Indeed, the data imply that although collagen gels offer an attractive model system with which to rapidly assess the effect of modulating ECM stiffness on cellular behavior in a 3D context, several confounding variables seriously compromise any ability to rigorously isolate and interpret the effect of matrix stiffness per se on cellular behavior using this hydrogel model.

Self Assembling Peptides (SAP): Flexible, Protein-absorbing, Synthetic Matrix that Mimic Collagen Architecture

A number of materials are readily available whose elasticity can be dynamically modulated by maintaining ligand binding constant. Materials such as hyaluronic acid, poly(ethylene) glycol, and polyglycolic acid can be modified to provide rigorously controlled biochemical cues [46, 68–74]. Unfortunately, the architecture of these materials is strikingly different from that of natural ECMs such as type I collagen, thereby compromising their utility as natural ECM substrates. By contrast, self assembling peptide hydrogels (SAPs) are biocompatible synthetic substrates that not only mimic the micro-architecture of natural collagen gels (Fig 2C) but lend themselves to chemical modification. SAPs are composed of 16 repeating amino acid residues (alternating hydrophilic and hydrophobic chains) that self-assemble to form nano fibers under physiological salt conditions due to hydrophobic (between alanines) and ionic bonding (between arginine and aspartic acid residues) between the amino acids [55]. Although SAPs can be mechanically tethered with ligand [59, 75], these peptides are also protein-adsorbing [76]. Thus, although they do not contain integrin-binding sites, and therefore they cannot mediate ligand-dependent ECM receptor signaling, they can be readily conjugated, tethered, or adsorbed with quantifiable concentrations of ligand via direct peptide conjugation or through ECM protein adsorption. Moreover, by varying the concentration of the SAP, the stiffness of the gel can be modulated over a physiologically appropriate range to achieve a visco elasticity similar to soft tissues such as a healthy breast on the one hand and a cancerous breast on the other hand [8, 77–79].

To explore the utility of SAPs as biocompatible materials for exploring the effect of ECM stiffness on epithelial morphogenesis and homeostasis we characterized the physical

topology and mechanical properties of one of these commercially available SAPs gels, PuraMatrix, over the range of visco elasticity deemed useful for the study of normal and transformed epithelial behavior. We found that varying SAP concentration from 1.2–3.2 mg/mL generated a Young's modulus that ranged from 120–1,200 Pa, analogous to what we were able to achieve by varying collagen concentration from 1.2–3.2 mg/mL (Fig 2B and 2D). Importantly, SEM analysis revealed that unlike collagen I gels, SAPs gel micro-architecture did not substantially change within this stiffness range and gel concentration. Indeed, we noted that pore size only varied by approximately 10% and fibril topology remained within the range of 45–75 nm even when gel contraction was varied from 1.2–3.2 mg/mL (Fig 2E-F). By contrast the pore size of the collagen gels varied by over 30% and fibril topology ranged from 50 to 170 μm when collagen concentration was modified across this same range (Fig 2E-F). Curiously, although we detected no statistically-significant differences in the overall fiber organization and matrix topology as a function of SAPs gel concentration and stiffness, we did quantify a modest, but consistent increase in peptide mass per volume (data not shown). The fact that the observed difference was only a 10% increase in the fraction of soluble peptide at the highest gel concentration indicates that the elevated gel stiffness likely reflects a subtle increase in either the fiber diameter, length, or absolute number. In this respect, we determined that the projected pore size and overall fiber mesh did not change drastically, suggesting that SAP gel stiffness was more than likely due to an increase in fiber diameter and/or enhanced fiber density. Indeed, there was a positive but-insignificant trend between SAP stiffness and decreased projected pore size and increased fiber thickness. The fact that we could not accurately document changes in these variables is more than likely due to the resolution limitation of our detection method which is unable to detect such subtle nano-scale differences in fiber diameter and pore size variability. Consistently, the stiffness of a fibrous material can be largely attributed to the sum of the bending moments of all the fibers. Second moment of inertia is a shape property that can be used to predict deflections and stresses in the beams/fibers, which would be representative of its bulk stiffness. Assuming a circular cross-section of the fibers, the moment of inertia, I_o, would be proportional to the radius raised to the 4^{th} power ($I_o = \pi r^2/4$), such that incredibly small changes in the radius would be reflected by an increased capacity to dramatically alter the bendability or stiffness of the material. In these studies we observed an approximate six fold increase in gel stiffness between the soft and the stiff SAPs gels which can easily be accounted for by a mere a 2 nm change in fiber thickness. As such, the theoretical differences between soft and stiff SAP gels are well beyond the 3–5 nm resolution capacity of SEM imaging. Moreover and importantly, despite the fact that it is obvious that SAP morphology must vary to some degree as a function of gel concentration/stiffness, the magnitude of such a modest nanometer-scale variation would exert a negligible effect on cellular functions, such as migration and invasion, because cells operate on a length scale of 10–50 μm. Instead, variations in pore and fiber diameter within the tens to hundreds of nanometers, which is comparable to what we quantified for collagen gels of increasing concentration/ stiffness, are likely to significantly alter cellular invasion and migration. These findings suggest that SAPs gels could provide a viable alternative ECM for studying the effect of ECM rigidity on epithelial invasive phenotype in a 3D context.

SAP Gels Support Epithelial Morphogenesis and Direct Apical-Basal Tissue Polarity

To explore the utility of SAP gels as a tractable matrix system for studying the interplay between ECM stiffness and epithelial cell behavior in 3D, we grew MECs within un-conjugated, compliant, SAP gels in the absence of adsorbed ECM protein. We noted that MECs embedded within SAP gels survived and grew to assemble epithelial colonies. However, colony size was non-uniform and immuno-fluorescence analysis revealed that the colonies lacked polarity (data not shown). We therefore supplemented the SAP gels with laminin (100 μg/mL) or rBM (2 mg/mL; 10%) and assayed for effects on MEC growth,

survival, and multi-cellular morphogenesis. Analogous to MECs embedded within rBM or a mixture of collagen I and rBM, MECs embedded within the laminin- or rBM-supplemented SAP gels proliferated rapidly for the first 5–6 days after which they growth-arrested, as revealed by loss of Ki-67 immuno-staining and the maintenance of a stable colony diameter, and initiated tissue morphogenesis, as indicated by elevated numbers of cells in the center of the colonies positive for activated caspase 3 (Fig 3B, Fig 4C and 4D). Consistently, MEC colonies generated in the laminin-supplemented SAPs gels assembled acini with cleared lumens that had similar diameters to those generated in rBM and collagen I/rBM gels (Fig 3A and 3C, quantified in 3B). Moreover, acini generated in the laminin-supplemented SAP gels achieved apical-basal polarity, as revealed by basally localized β4 integrin (Fig 3D, left panel, see arrow), basal-lateral β1 integrin, and cell-cell localized β-catenin (Fig 3D, middle and right panels, see arrows). These phenotypes are analogous to those observed in rBM or in 1.2 mg/mL collagen I gels supplemented with laminin or rBM (Fig 1A). Moreover, and importantly, similar to what we and others have routinely observed using rBM gels, SAP gels were able to support stable acini development as revealed by uniform colony differentiation and repression of genes that compromise acini stability and differentiation, such as fibronectin (Fig 3D, right panel; Fig 4E-F). These findings indicate that compliant SAP gels, when supplemented with the appropriate biochemical ECM cues, can support normal MEC growth and viability and direct multi-cellular tissue morphogenesis.

Modulating SAP Stiffness Perturbs Epithelial Morphogenesis, Disrupts Apical-Basal Tissue Polarity, and Induces Pro-tumor Gene Expression

We next asked whether increasing SAPs gel stiffness could perturb MEC morphogenesis and tissue integrity to induce a tumor-like phenotype. MECs were embedded within 1.2-3.2 mg/mL SAPs gels at concentrations that generated mechanical properties (Young's modulus) that recapitulated what we previously measured for normal and early stage breast tumor tissue, respectively [10] (Fig 2D). Similar to MECs within rBM gels, MEC colonies embedded within highly compliant laminin-supplemented SAPs assembled growth-arrested acini that showed negligible Ki-67 staining by day 10 of culture (Fig 4C and 4D). Mammary acini within soft SAPs also consistently cleared their lumens, likely through induction of apoptosis in the cells lacking contact with the protein-adsorbed SAPs gels, as revealed by elevated numbers of cells within the day 10–12 colony lumens with activated caspase 3 staining (Fig 4B). By contrast, MEC colonies embedded within rigid SAP gels continued to proliferate, as revealed by elevated Ki-67 staining throughout the colony (Fig 4D), showed negligible death of the cells within the center of the colony, as revealed by reduced activated caspase 3 positive cells in the center of the colonies (Fig 4C), and consequently failed to clear their lumens (Fig 4A-B). The colonies assembled within the rigid SAPs also lacked apical-basal polarity, as revealed by highly diffuse β-catenin and β1 integrin (Fig 4E). Intriguingly, we noted that the MECs embedded within the stiff SAPs matrix also showed severely compromised colony integrity, as revealed by gross disorganization of the colony and individual MECs disseminating away from the colony and invading into the surrounding matrix (Fig 4E). These findings imply that matrix stiffness "per se" may in fact promote cell invasion given the appropriate matrix context and cell state. In this regard, by way of a plausible mechanism, we noted that SAP stiffness induced the expression of two genes implicated in tumor progression and invasion, fibronectin 1 and EGFR (Fig 4F), and additionally enhanced fibronectin 1 deposition by the MECs embedded within the gel (Fig 4E-F).

Discussion

We exploited the unique properties of one SAP gel (PuraMatrix) to study the interplay between ECM stiffness and multi-cellular epithelial morphogenesis and transformation.

SAPs gels provide a versatile model system with tunable mechanical properties and a native-like ECM fibril morphology. We were able to show that 3D laminin- or rBM- adsorbed compliant SAPs gels are able to recapitulate MEC morphogenesis and that a stiff SAPs gel disrupts tissue architecture, compromises tissue polarity and induces fibronectin and EGFR expression to promote an invasive, tumor-like phenotype without substantially altering ECM topology, pore size, and ligand density. Thus, we maintain that this matrix is a defined and tractable system that could be used to definitively study the effect of ECM tension on multicellular epithelial cell behavior in a 3D tissue-like context. The availability of such a versatile system could have profound clinical implications by permitting the execution of experiments aimed at clarifying the biophysically-driven changes in tissue phenotype and molecular signature associated with tumor progression. One could imagine using this system for high throughput drug screening to identify novel therapeutics that would provide improved, personalized cancer therapeutics designed to not only target tumor cells but also to treat their phenotypic response to modifications in their surrounding ECM.

Unlike natural gels which exhibit striking changes in architecture, decreased pore size and altered ligand density as matrix stiffness is increased, SAP gels offer a tractable system with which to vary ECM stiffness over a dynamic range without significantly affecting any of these variables. In this regard, while other synthetic systems, including HA gels and PEG gels, have been adapted to study the effect of ECM rigidity on cell and tissue behavior these substrates fail to recapitulate the topology of natural matrices, cannot be remodeled without conjugation of collagenase digestible peptides, and often limit invasion due to minute pore size features (unpublished findings). Two major approaches for engineering *in vitro* systems with tunable mechanical properties have been the conjugation of cell-compatible adhesion peptides into synthetic matrices [48, 80–82] or the application of biophysically-modified natural matrices (e.g. varying collagen gel concentration and/or cross-linking). Synthetic matrices allow for a robust control of ligand density as a function of stiffness however, they typically fail to recapitulate the appropriate topological cues programmed in the networks of natural materials. On the other hand, natural materials offer physiologically-relevant architectures, but introduce an array of confounding biophysical cues when concentration is varied or cross-linking status is changed (as means to vary stiffness). This includes profound effects on ligand density, fiber diameter, pore size, and overall micro-architecture. These complicating variables are not insignificant in that cells are able to sense and respond to matrix topology and presentation [83–87]. For instance, tumors show elevated contractility and enhanced crosstalk with stromal fibroblasts in response to changes in matrix topology and this perturbed dialogue promotes tension-dependent remodeling and linearization of collagen fibers that promote an invasive tumor matrix that can foster metastasis [88–89]. Thus, due to a myriad of limitations endemic to current *in vitro* systems, the issue as to whether or not ECM compliance per se can modulate tissue morphology and transformation (as well as the identification of molecular mechanisms that drive these phenomena) remains unresolved. In this regard, the SAP system described here has a multitude of positive features that might overcome many of these limitations, and while mechanical fragility remains one challenge when manipulating these gels, their net benefit at present far outweighs this minor experimental difficulty.

Prior studies using 3D collagen gels with increasing concentration and/or elevated collagen cross-links (and hence stiffness) indicate that ECM stiffness perturbs multi-cellular epithelial morphogenesis but fails to induce invasion unless combined with elevated growth factor or oncogenic signaling [3, 10]. Such findings imply that ECM stiffness collaborates with oncogenes to drive tumor progression and argue that stiffness is a tumor promoter rather than initiator. We noted that elevating SAP stiffness was sufficient to drive epithelial invasion suggesting stiffness alone could promote cell invasion. One plausible explanation for why prior studies failed to demonstrate invasion causality through ECM stiffness is that

stiffened collagen gels (mediated through elevated protein concentration or cross-linking) simultaneously decrease pore size and limit growth factor diffusion, thereby complicating data interpretation because these variables would themselves impede and delay migration. Indeed, prior studies suggest that stiffer collagen or fibrin gels can in fact reduce the rate of cell migration and that migration within such gels relies critically on MMP-dependent matrix remodeling to permit tumor cell invasion [90–92]. Yet, ECM stiffness promotes invadopodia [92–94] and modulates integrin adhesion dynamics [23, 64, 95–96]. Furthermore, ECM rigidity enhances cell contractility to enhance cell motility and promotes invasion through ECM reorganization and alignment, suggesting ECM stiffness should promote and not impede invasion. These findings indicate that ECM stiffness could be both a tumor promoter and initiator; a possibility that now needs to be rigorously addressed. In this regard, SAP gels could prove instrumental in addressing this intriguing possibility.

In conclusion, tumor progression is associated with loss of tissue organization and disassembly of multicellular tissue structures. We observed that compliant laminin-supplemented SAPs gels are able to support MEC acini morphogenesis and that a stiff SAPs gel perturbs tissue polarity, destabilizes cell-cell adhesions and increases the expression of tumor promoting genes including fibronectin and the EGF receptor. These findings are consistent with the notion that ECM rigidity per se, in conjunction with appropriate architecture, could promote tumor progression through destabilization of tissue architecture; a findings that we now stand prepared to investigate using the SAP system of epithelial morphogenesis.

Acknowledgments

We thank C. Frantz and J. Lakins for technical assistance. This work was supported by an NCI U54CA143836-01 grant to J. Liphardt and V.M.W., and 5R01CA138818-02 to V.M.W., a Department of Defense Breast Cancer Research Era of Hope Scholar award W81XWH-05-1-330 to V.M.W. and a National Science Foundation (GRFP) Fellowship to Y.A.M.

References

1. Ingber DE. Mechanical control of tissue morphogenesis during embryological development. Int J Dev Biol. 2006; 50(2–3):255–66. [PubMed: 16479493]
2. Yu H, Mouw JK, Weaver VM. Forcing form and function: biomechanical regulation of tumor evolution. Trends Cell Biol. 2010
3. Engler AJ, et al. Matrix elasticity directs stem cell lineage specification. Cell. 2006; 126(4):677–89. [PubMed: 16923388]
4. Engler AJ, et al. Embryonic cardiomyocytes beat best on a matrix with heart-like elasticity: scar-like rigidity inhibits beating. J Cell Sci. 2008; 121(Pt 22):3794–802. [PubMed: 18957515]
5. Klocke R, et al. Arterial stiffness and central blood pressure, as determined by pulse wave analysis, in rheumatoid arthritis. Ann Rheum Dis. 2003; 62(5):414–8. [PubMed: 12695151]
6. Flanagan LA, et al. Neurite branching on deformable substrates. Neuroreport. 2002; 13(18):2411–5. [PubMed: 12499839]
7. Flanagan LA, Ju YE, Janmey PA. Growth and branching of neuronal processes on deformable substrates. Molecular Biology of the Cell. 2000; 11:458.
8. Levental KR, et al. Matrix Crosslinking Forces Tumor Progression by Enhancing Integrin signaling. CELL. 2009 In Press.
9. Paszek MJ V, Weaver M. The tension mounts: mechanics meets morphogenesis and malignancy. J Mammary Gland Biol Neoplasia. 2004; 9(4):325–42. [PubMed: 15838603]
10. Paszek MJ, et al. Tensional homeostasis and the malignant phenotype. Cancer Cell. 2005; 8(3): 241–254. [PubMed: 16169468]
11. Pelham RJ Jr, Wang Y. Cell locomotion and focal adhesions are regulated by substrate flexibility. Proc Natl Acad Sci U S A. 1997; 94(25):13661–5. [PubMed: 9391082]

12. Yeung T, et al. Effects of substrate stiffness on cell morphology, cytoskeletal structure, and adhesion. Cell Motil Cytoskeleton. 2005; 60(1):24–34. [PubMed: 15573414]
13. Wong JY, et al. Directed Movement of Vascular Smooth Muscle Cells on Gradient-Compliant Hydrogels. Langmuir. 2003; 19(5):1908–1913.
14. Gaudet C, et al. Influence of type I collagen surface density on fibroblast spreading, motility, and contractility. Biophys J. 2003; 85(5):3329–35. [PubMed: 14581234]
15. Heidemann SR, Wirtz D. Towards a regional approach to cell mechanics. Trends Cell Biol. 2004; 14(4):160–6. [PubMed: 15066633]
16. Discher DE, Janmey P, Wang YL. Tissue cells feel and respond to the stiffness of their substrate. Science. 2005; 310(5751):1139–43. [PubMed: 16293750]
17. Engler AJ, et al. Myotubes differentiate optimally on substrates with tissue-like stiffness: pathological implications for soft or stiff microenvironments 10.1083/jcb.200405004. J Cell Biol. 2004; 166(6):877–887. [PubMed: 15364962]
18. Reinhart-King CA, Dembo M, Hammer DA. Cell-cell mechanical communication through compliant substrates. Biophys J. 2008; 95(12):6044–51. [PubMed: 18775964]
19. Califano, JP.; Reinhart-King, CA. The effects of substrate elasticity on endothelial cell network formation and traction force generation. Conf Proc IEEE Eng Med Biol Soc; 2009; 2009. p. 3343-5.
20. Khatiwala CB, et al. ECM compliance regulates osteogenesis by influencing MAPK signaling downstream of RhoA and ROCK. J Bone Miner Res. 2009; 24(5):886–98. [PubMed: 19113908]
21. Gardel ML, et al. Traction stress in focal adhesions correlates biphasically with actin retrograde flow speed. J Cell Biol. 2008; 183(6):999–1005. [PubMed: 19075110]
22. Pasapera AM, et al. Myosin II activity regulates vinculin recruitment to focal adhesions through FAK-mediated paxillin phosphorylation. J Cell Biol. 2010; 188(6):877–90. [PubMed: 20308429]
23. Gardel ML, et al. Mechanical integration of actin and adhesion dynamics in cell migration. Annu Rev Cell Dev Biol. 2010; 26:315–33. [PubMed: 19575647]
24. Lee JS, et al. Ballistic intracellular nanorheology reveals ROCK-hard cytoplasmic stiffening response to fluid flow. J Cell Sci. 2006; 119(Pt 9):1760–8. [PubMed: 16636071]
25. Khatau SB, et al. A perinuclear actin cap regulates nuclear shape. Proc Natl Acad Sci U S A. 2009; 106(45):19017–22. [PubMed: 19850871]
26. Lee JS, et al. Nuclear lamin A/C deficiency induces defects in cell mechanics, polarization, and migration. Biophys J. 2007; 93(7):2542–52. [PubMed: 17631533]
27. Spencer VA, Xu R, Bissell MJ. Gene expression in the third dimension: the ECM-nucleus connection. J Mammary Gland Biol Neoplasia. 2010; 15(1):65–71. [PubMed: 20107877]
28. Boudreau N, Werb Z, Bissell MJ. Suppression of apoptosis by basement membrane requires three-dimensional tissue organization and withdrawal from the cell cycle. Proc Natl Acad Sci U S A. 1996; 93(8):3509–13. [PubMed: 8622967]
29. Wang F, et al. Phenotypic reversion or death of cancer cells by altering signaling pathways in three-dimensional contexts. J Natl Cancer Inst. 2002; 94(19):1494–503. [PubMed: 12359858]
30. Weaver VM, et al. Reversion of the malignant phenotype of human breast cells in three-dimensional culture and in vivo by integrin blocking antibodies. J Cell Biol. 1997; 137(1):231–45. [PubMed: 9105051]
31. Weaver VM, et al. The importance of the microenvironment in breast cancer progression: recapitulation of mammary tumorigenesis using a unique human mammary epithelial cell model and a three-dimensional culture assay. Biochem Cell Biol. 1996; 74(6):833–51. [PubMed: 9164652]
32. Pedersen JA, Swartz MA. Mechanobiology in the third dimension. Ann Biomed Eng. 2005; 33(11):1469–90. [PubMed: 16341917]
33. Pampaloni F, Reynaud EG, Stelzer EH. The third dimension bridges the gap between cell culture and live tissue. Nat Rev Mol Cell Biol. 2007; 8(10):839–45. [PubMed: 17684528]
34. Weaver VM, et al. beta4 integrin-dependent formation of polarized three-dimensional architecture confers resistance to apoptosis in normal and malignant mammary epithelium. Cancer Cell. 2002; 2(3):205–16. [PubMed: 12242153]

35. Zahir N V, Weaver M. Death in the third dimension: apoptosis regulation and tissue architecture. Curr Opin Genet Dev. 2004; 14(1):71–80. [PubMed: 15108808]
36. Jacks T, Weinberg RA. Taking the study of cancer cell survival to a new dimension. Cell. 2002; 111(7):923–5. [PubMed: 12507419]
37. Tse JR, Engler AJ. Stiffness gradients mimicking in vivo tissue variation regulate mesenchymal stem cell fate. PLoS One. 2011; 6(1):e15978. [PubMed: 21246050]
38. Provenzano PP, et al. Collagen density promotes mammary tumor initiation and progression. BMC Med. 2008; 6:11. [PubMed: 18442412]
39. Barcellos-Hoff MH, et al. Functional differentiation and alveolar morphogenesis of primary mammary cultures on reconstituted basement membrane. Development. 1989; 105(2):223–35. [PubMed: 2806122]
40. Foster CS, et al. Human mammary gland morphogenesis in vitro: the growth and differentiation of normal breast epithelium in collagen gel cultures defined by electron microscopy, monoclonal antibodies, and autoradiography. Dev Biol. 1983; 96(1):197–216. [PubMed: 6825953]
41. Richards J, et al. Response of end bud cells from immature rat mammary gland to hormones when cultured in collagen gel. Exp Cell Res. 1983; 147(1):95–109. [PubMed: 6352291]
42. Emerman JT, Burwen SJ, Pitelka DR. Substrate properties influencing ultrastructural differentiation of mammary epithelial cells in culture. Tissue Cell. 1979; 11(1):109–19. [PubMed: 572104]
43. Chalupowicz DG, et al. Fibrin II induces endothelial cell capillary tube formation. J Cell Biol. 1995; 130(1):207–15. [PubMed: 7540617]
44. Ghajar CM, et al. The effect of matrix density on the regulation of 3-D capillary morphogenesis. Biophys J. 2008; 94(5):1930–41. [PubMed: 17993494]
45. Roeder BA, et al. Tensile mechanical properties of three-dimensional type I collagen extracellular matrices with varied microstructure. J Biomech Eng. 2002; 124(2):214–22. [PubMed: 12002131]
46. Ulrich TA, et al. Probing cellular mechanobiology in three-dimensional culture with collagen-agarose matrices. Biomaterials. 2010; 31(7):1875–84. [PubMed: 19926126]
47. Lutolf MP, et al. Synthetic matrix metalloproteinase-sensitive hydrogels for the conduction of tissue regeneration: engineering cell-invasion characteristics. Proc Natl Acad Sci U S A. 2003; 100(9):5413–8. [PubMed: 12686696]
48. Seliktar D, et al. MMP-2 sensitive, VEGF-bearing bioactive hydrogels for promotion of vascular healing. J Biomed Mater Res A. 2004; 68(4):704–16. [PubMed: 14986325]
49. Schmedlen RH, Masters KS, West JL. Photocrosslinkable polyvinyl alcohol hydrogels that can be modified with cell adhesion peptides for use in tissue engineering. Biomaterials. 2002; 23(22): 4325–32. [PubMed: 12219822]
50. Mann BK, West JL. Cell adhesion peptides alter smooth muscle cell adhesion, proliferation, migration, and matrix protein synthesis on modified surfaces and in polymer scaffolds. J Biomed Mater Res. 2002; 60(1):86–93. [PubMed: 11835163]
51. Kloxin AM, et al. Photodegradable hydrogels for dynamic tuning of physical and chemical properties. Science. 2009; 324(5923):59–63. [PubMed: 19342581]
52. DeForest CA, Polizzotti BD, Anseth KS. Sequential click reactions for synthesizing and patterning three-dimensional cell microenvironments. Nat Mater. 2009; 8(8):659–64. [PubMed: 19543279]
53. Caplan MR, et al. Control of self-assembling oligopeptide matrix formation through systematic variation of amino acid sequence. Biomaterials. 2002; 23(1):219–27. [PubMed: 11762841]
54. Zhang S, et al. Self-complementary oligopeptide matrices support mammalian cell attachment. Biomaterials. 1995; 16(18):1385–93. [PubMed: 8590765]
55. Sieminski AL, et al. The stiffness of three-dimensional ionic self-assembling peptide gels affects the extent of capillary-like network formation. Cell Biochem Biophys. 2007; 49(2):73–83. [PubMed: 17906362]
56. Gelain F, et al. Designer self-assembling peptide nanofiber scaffolds for adult mouse neural stem cell 3-dimensional cultures. PLoS One. 2006; 1:e119. [PubMed: 17205123]

57. Horii A, et al. Biological designer self-assembling peptide nanofiber scaffolds significantly enhance osteoblast proliferation, differentiation and 3-D migration. PLoS One. 2007; 2(2):e190. [PubMed: 17285144]
58. Wang S, et al. Three-Dimensional Primary Hepatocyte Culture in Synthetic Self-Assembling Peptide Hydrogel. Tissue Eng. 2008
59. Genove E, et al. Functionalized self-assembling peptide hydrogel enhance maintenance of hepatocyte activity in vitro. J Cell Mol Med. 2009; 13(9B):3387–97. [PubMed: 19912437]
60. Johnson KR, Leight JL, Weaver VM. Demystifying the effects of a three-dimensional microenvironment in tissue morphogenesis. Methods Cell Biol. 2007; 83:547–83. [PubMed: 17613324]
61. Zahir N, et al. Autocrine laminin-5 ligates alpha6beta4 integrin and activates RAC and NFkappaB to mediate anchorage-independent survival of mammary tumors. J Cell Biol. 2003; 163(6):1397–407. [PubMed: 14691145]
62. Gudjonsson T, et al. Normal and tumor-derived myoepithelial cells differ in their ability to interact with luminal breast epithelial cells for polarity and basement membrane deposition. J Cell Sci. 2002; 115(Pt 1):39–50. [PubMed: 11801722]
63. Lopez, et al. 2010 (in revision).
64. Fischer RS, et al. Local cortical tension by myosin II guides 3D endothelial cell branching. Curr Biol. 2009; 19(3):260–5. [PubMed: 19185493]
65. Zaman MH, Matsudaira P, Lauffenburger DA. Understanding effects of matrix protease and matrix organization on directional persistence and translational speed in three–dimensional cell migration. Ann Biomed Eng. 2007; 35(1):91–100. [PubMed: 17080315]
66. Kim HD, et al. Epidermal growth factor-induced enhancement of glioblastoma cell migration in 3D arises from an intrinsic increase in speed but an extrinsic matrix- and proteolysis-dependent increase in persistence. Mol Biol Cell. 2008; 19(10):4249–59. [PubMed: 18632979]
67. Provenzano PP, et al. Contact guidance mediated three-dimensional cell migration is regulated by Rho/ROCK-dependent matrix reorganization. Biophys J. 2008; 95(11):5374–84. [PubMed: 18775961]
68. Cima LG, et al. Hepatocyte culture on biodegradable polymeric substrates. Biotechnol Bioeng. 1991; 38(2):145–58. [PubMed: 18600745]
69. Cima LG, et al. Tissue engineering by cell transplantation using degradable polymer substrates. J Biomech Eng. 1991; 113(2):143–51. [PubMed: 1652042]
70. Domansky K, et al. Perfused multiwell plate for 3D liver tissue engineering. Lab Chip. 2010; 10(1):51–8. [PubMed: 20024050]
71. Burdick JA, Anseth KS. Photoencapsulation of osteoblasts in injectable RGD-modified PEG hydrogels for bone tissue engineering. Biomaterials. 2002; 23(22):4315–23. [PubMed: 12219821]
72. Hoque ME, et al. Fabrication using a rapid prototyping system and in vitro characterization of PEG-PCL-PLA scaffolds for tissue engineering. J Biomater Sci Polym Ed. 2005; 16(12):1595–610. [PubMed: 16366339]
73. Brigham MD, et al. Mechanically robust and bioadhesive collagen and photocrosslinkable hyaluronic acid semi-interpenetrating networks. Tissue Eng Part A. 2009; 15(7):1645–53. [PubMed: 19105604]
74. Chung C, et al. The influence of degradation characteristics of hyaluronic acid hydrogels on in vitro neocartilage formation by mesenchymal stem cells. Biomaterials. 2009; 30(26):4287–96. [PubMed: 19464053]
75. Genove E, et al. The effect of functionalized self-assembling peptide scaffolds on human aortic endothelial cell function. Biomaterials. 2005; 26(16):3341–51. [PubMed: 15603830]
76. Sieminski AL, et al. Primary sequence of ionic self-assembling peptide gels affects endothelial cell adhesion and capillary morphogenesis. J Biomed Mater Res A. 2008; 87(2):494–504. [PubMed: 18186067]
77. Paszek MJ, et al. Tensional homeostasis and the malignant phenotype. Cancer Cell. 2005; 8(3): 241–54. [PubMed: 16169468]
78. Beil M, et al. Sphingosylphosphorylcholine regulates keratin network architecture and visco-elastic properties of human cancer cells. Nat Cell Biol. 2003; 5(9):803–11. [PubMed: 12942086]

79. Colpaert C, et al. The presence of a fibrotic focus is an independent predictor of early metastasis in lymph node-negative breast cancer patients. Am J Surg Pathol. 2001; 25(12):1557–8. [PubMed: 11717549]
80. Peyton SR, et al. The use of poly(ethylene glycol) hydrogels to investigate the impact of ECM chemistry and mechanics on smooth muscle cells. Biomaterials. 2006; 27(28):4881–93. [PubMed: 16762407]
81. Peyton SR, et al. The effects of matrix stiffness and RhoA on the phenotypic plasticity of smooth muscle cells in a 3-D biosynthetic hydrogel system. Biomaterials. 2008; 29(17):2597–607. [PubMed: 18342366]
82. Patterson J, Hubbell JA. Enhanced proteolytic degradation of molecularly engineered PEG hydrogels in response to MMP-1 and MMP-2. Biomaterials. 2010; 31(30):7836–45. [PubMed: 20667588]
83. Ayala P, Lopez JI, Desai TA. Microtopographical cues in 3D attenuate fibrotic phenotype and extracellular matrix deposition: implications for tissue regeneration. Tissue Eng Part A. 2010; 16(8):2519–27. [PubMed: 20235832]
84. Collins JM, et al. Three-dimensional culture with stiff microstructures increases proliferation and slows osteogenic differentiation of human mesenchymal stem cells. Small. 2010; 6(3):355–60. [PubMed: 19943257]
85. Bernards DA, Desai TA. Nanotemplating of biodegradable polymer membranes for constant-rate drug delivery. Adv Mater. 2010; 22(21):2358–62. [PubMed: 20376851]
86. Choquet D, Felsenfeld DP, Sheetz MP. Extracellular matrix rigidity causes strengthening of integrin-cytoskeleton linkages. Cell. 1997; 88(1):39–48. [PubMed: 9019403]
87. Chen CS, et al. Geometric control of cell life and death. Science. 1997; 276(5317):1425–8. [PubMed: 9162012]
88. Provenzano PP, et al. Collagen reorganization at the tumor-stromal interface facilitates local invasion. BMC Med. 2006; 4(1):38. [PubMed: 17190588]
89. Rhee S, Grinnell F. Fibroblast mechanics in 3D collagen matrices. Adv Drug Deliv Rev. 2007; 59(13):1299–305. [PubMed: 17825456]
90. Harley BA, et al. Microarchitecture of three-dimensional scaffolds influences cell migration behavior via junction interactions. Biophys J. 2008; 95(8):4013–24. [PubMed: 18621811]
91. Zaman MH, et al. Computational model for cell migration in three-dimensional matrices. Biophys J. 2005; 89(2):1389–97. [PubMed: 15908579]
92. Zaman MH, et al. Migration of tumor cells in 3D matrices is governed by matrix stiffness along with cell-matrix adhesion and proteolysis. Proc Natl Acad Sci U S A. 2006; 103(29):10889–94. [PubMed: 16832052]
93. Butcher DT, Alliston T, Weaver VM. A tense situation: forcing tumour progression. Nat Rev Cancer. 2009; 9(2):108–22. [PubMed: 19165226]
94. Albiges-Rizo C, et al. Actin machinery and mechanosensitivity in invadopodia, podosomes and focal adhesions. J Cell Sci. 2009; 122(Pt 17):3037–49. [PubMed: 19692590]
95. Stricker J, Falzone T, Gardel ML. Mechanics of the F-actin cytoskeleton. J Biomech. 2010; 43(1): 9–14. [PubMed: 19913792]
96. Borghi N, et al. Regulation of cell motile behavior by crosstalk between cadherin-and integrin-mediated adhesions. Proc Natl Acad Sci U S A. 2010; 107(30):13324–9. [PubMed: 20566866]

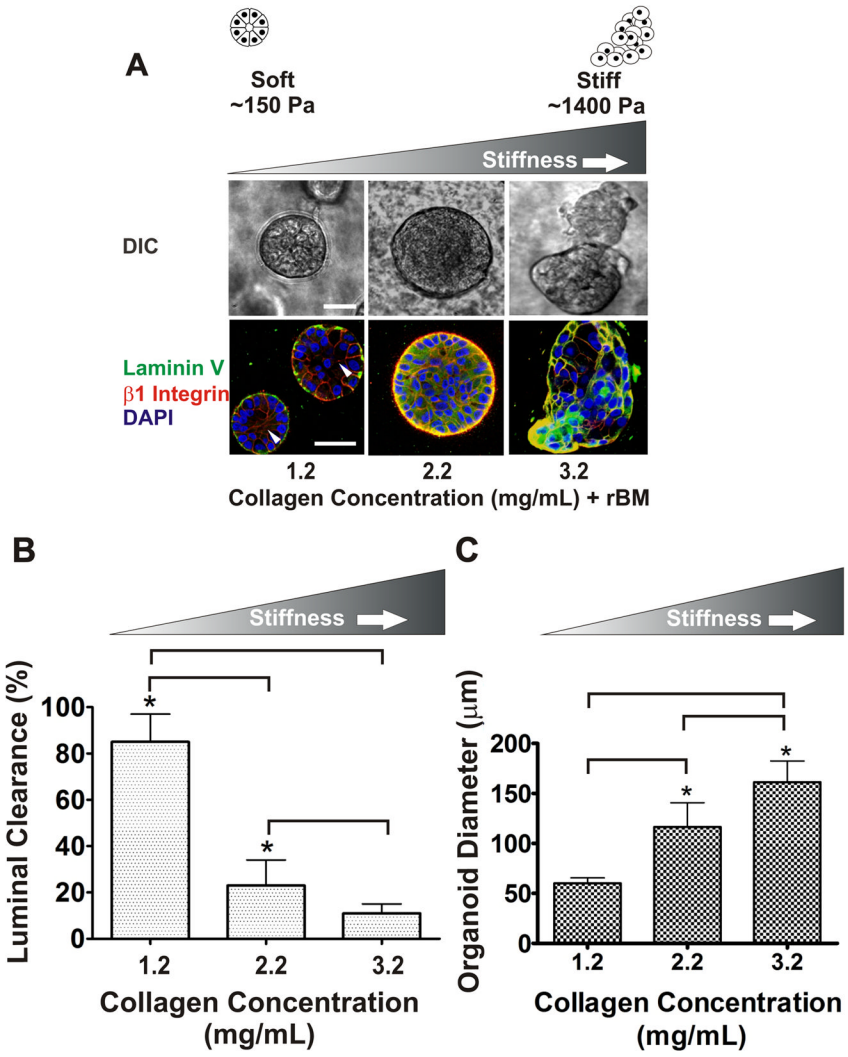

Figure 1. Increasing Collagen Concentration and Rigidity Stimulate Epithelial Growth and Survival and Compromise Tissue Morphogenesis and Integrity

A) (top) Phase contrast images of multi-cellular mammary epithelial cell (MEC) colonies embedded within type 1 collagen gels of increasing concentration (1.2–3.2 mg/mL) and stiffness (150–1400 Pa) for 12 days. Bar equals 30 μm. (bottom) Laser confocal immunofluorescence images of multi-cellular MEC colonies as above, stained for β1 integrin (red), laminin V (green), and nuclei (DAPI; blue). Bar equals 40 μm. **B)** Bar graphs showing quantification of luminal clearance measured in colonies shown in A. **C)** Bar graph showing average colony diameter of colonies shown in A. *indicates $p \leq 0.001$. Values shown in B- C represent mean ± SEM of multiple measurements from at least 3 independent experiments.

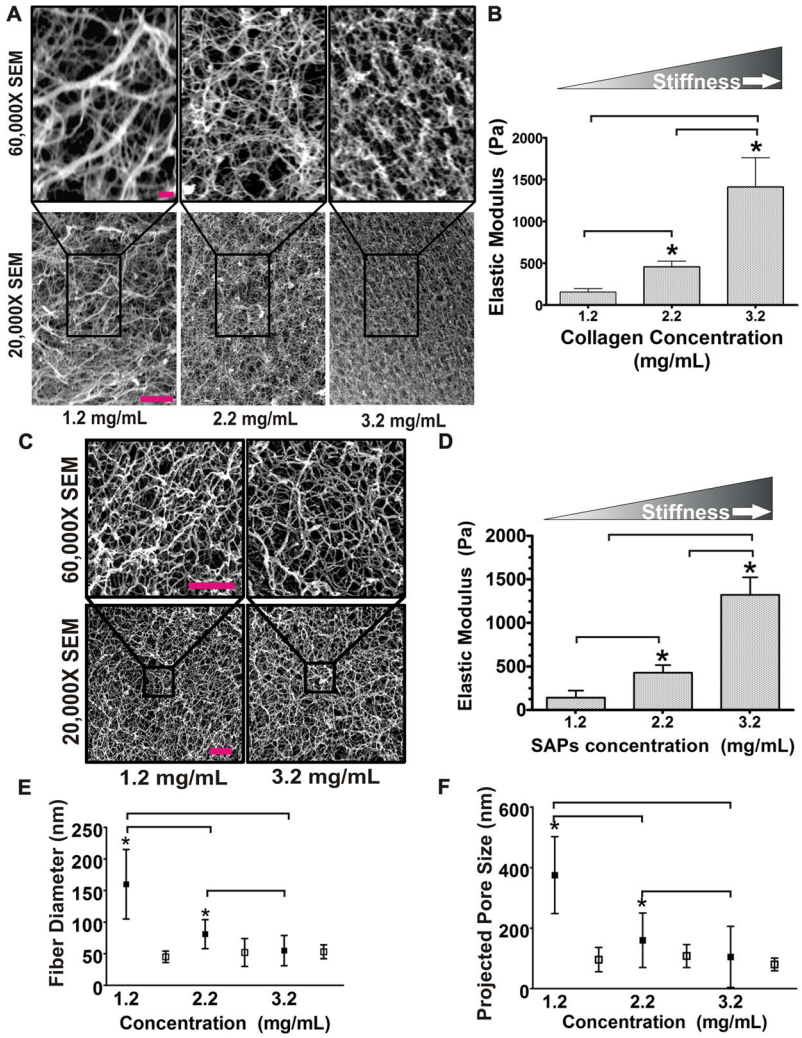

Figure 2. Self Assembling Peptides (SAP): Flexible, Protein-absorbing, Synthetic Matrix that Mimic Collagen Architecture

A) SEM microscopy images of collagen gels taken at high (top) and low (bottom) magnification illustrating the structural changes induced in collagen morphology, topology and pore size when collagen concentration is increased. Bar equals 5 μm. **B)** Bar graph quantifying Young's modulus of collagen gels of varying concentration as measured by shear rheology. **C)** SEM microscopy images of SAP gels taken at high (top) and low (bottom) magnification illustrating minimal structural changes in gel fiber morphology, topology and pore size when gel concentration is increased. Bar equals 200 nm. SEM resolution is 3–5nm (according to the manufacturer). **D)** Bar graphs quantifying SAP gel stiffness as a function of gel concentration as measured by shear rheology. **E)** Graphical depiction of fiber diameter quantified as a function of collagen (filled boxes) and SAP (open boxes) gel concentration. **F)** Graphical depiction of pore size measured as projected pore size in collagen (filled boxes) and SAP (open boxes) gels as a function of gel concentration. *indicates $p \leq 0.001$. Values shown in B and D-F represent mean ± SEM of multiple measurements from at least 3 independent experiments.

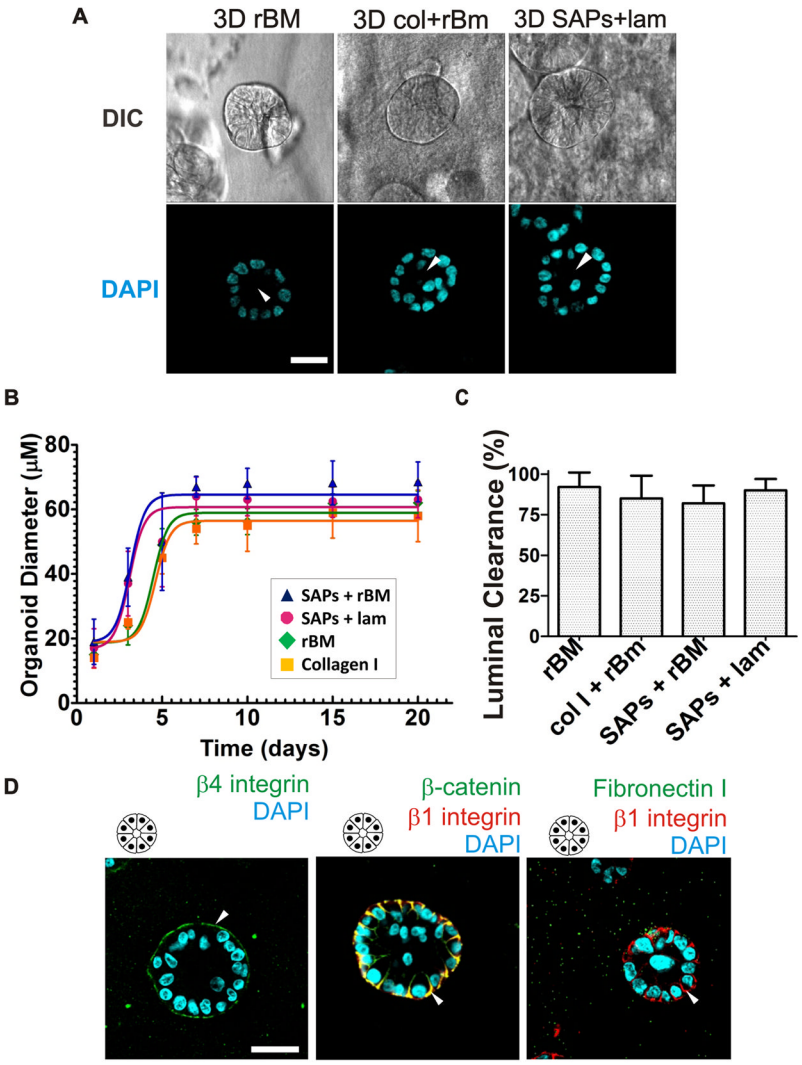

Figure 3. SAP Gels Support Epithelial Morphogenesis and Direct Apical-Basal Tissue Polarity

A) (top) Phase contrast images of representative multi-cellular MEC acini following growth within reconstituted basement membrane (rBM, Matrigel), type I collagen gels mixed with 10% rBM, or SAPs containing 100 μg/ml laminin for 20 days. (bottom) Laser confocal immunofluorescence images of cryosections (10 μm) of multi-cellular MEC colonies stained with DAPI to reveal nuclei (blue) showing presence of cleared lumens in acini generated in all gel conditions as described above. Bar equals 25 μm **B)** Line graphs showing growth curves for mammary colonies grown within rBM (green diamond), type 1 collagen gels mixed with 10% rBM (orange box) and SAPs supplemented either with laminin (red circle) or rBM (blue triangle). **C)** Bar graphs showing quantification of cleared lumens in mammary acini grown in rBM, type 1 collagen gels mixed with 10% rBM and SAPs supplemented either with laminin or rBM (differences in the diameters were not statistically significant). **D)** Laser confocal immunofluorescence images of cryosections (10 μm) of multi-cellular acini generated in SAPs supplemented with laminin stained with (left image) β4 integrin (green), (middle image) β-catenin (green) and β1 integrin (red) and (right image) fibronectin (green) and β1 integrin. All colonies were counter stained with DAPI (blue) to reveal nuclei. Bar equals 30 μm. Values shown in B and C represent mean ± SEM of multiple measurements from at least 3 independent experiments.

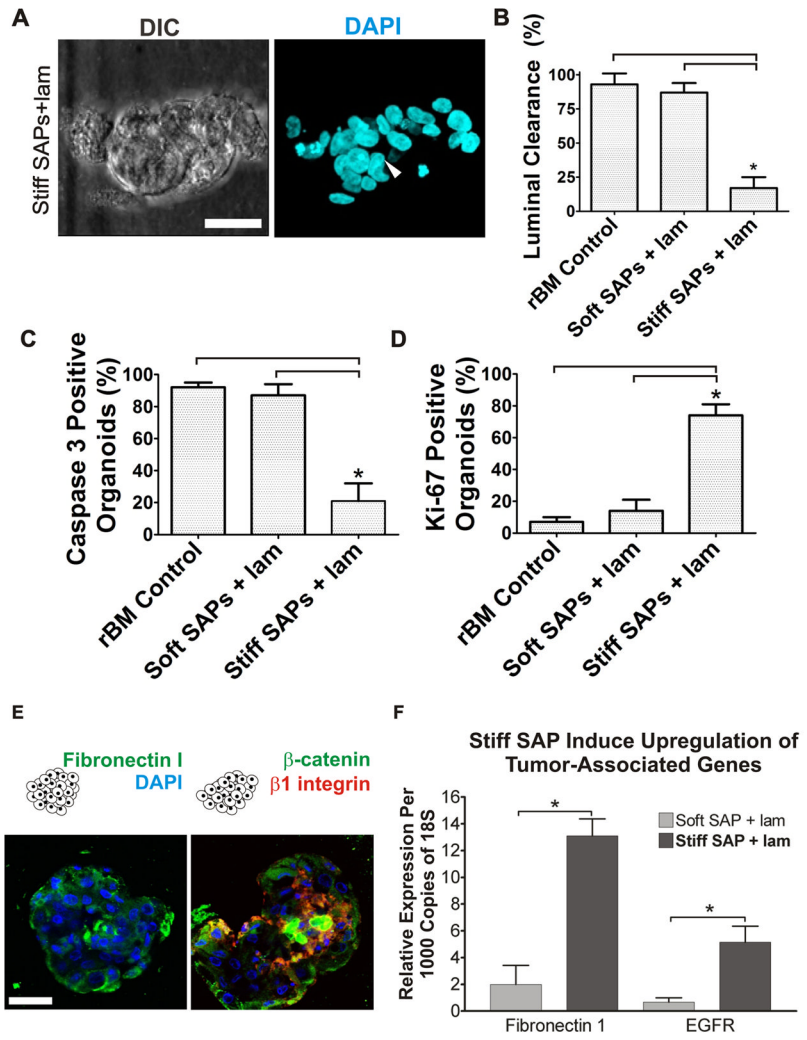

Figure 4. Modulating SAP Stiffness Perturbs Epithelial Morphogenesis, Disrupts Apical-Basal Tissue Polarity, and Alters Gene Expression

A) (left) Phase contrast images of representative multi-cellular MEC acini following growth within rigid SAPs containing 100 μg/ml laminin for 20 days. (right) Laser confocal immunofluorescence image of a cryosection (10 μm) of a multi-cellular MEC colony, generated as described above, stained with DAPI to reveal nuclei (blue) showing absence of cleared lumen in colony generated in a rigid SAP. Note the arrow pointing to the cells migrating into the stiff SAP gel suggestive of invasive behavior. Bar equals 25 μm. **B**) Bar graphs showing quantification of cleared lumens in mammary acini grown in rBM as compared to MEC colonies assembled in the soft and stiff SAPs supplemented with laminin. Note the high percent of luminal clearance quantified in the acini assembled in either the rBM gels or the compliant SAP gels and a significant reduction of cleared lumens quantified in the colonies generated in the stiff SAP gels. **C**) Bar graphs quantifying the number of caspase 3 positive lumens in colonies generated in rBM gels versus those assembled within compliant versus stiff SAP gels supplemented with laminin. Data indicate that SAP stiffness represses apoptosis in MECs. **D**) Bar graphs quantifying the number of Ki67 positive colonies detected in rBM gels versus those assembled within compliant versus stiff SAP gels supplemented with laminin. Data show that SAP stiffness promotes MEC proliferation. **D)** Laser confocal immunofluorescence showing representative image of cryosections (10 μm)

of a multi-cellular MEC colony generated in a stiff SAP supplemented with laminin that was stained with (left) fibronectin (green) and (right) β-catenin (green) and β1 integrin (red) and counter stained with DAPI (blue) to reveal nuclei. Bar equals 30 μm. F) Bar graphs showing the relative expression (by quantitative PCR) of fibronectin 1 and EGFR in acini isolated from soft and stiff laminin-supplemented SAP gels. Values shown in B-D and F represent mean ± SEM of multiple measurements from at least 3 independent experiments.